High purity trigonal selenium nanorods growth via laser ablation under controlled temperature

Zhi-Yuan Jiang, Zhao-Xiong Xie *, Su-Yuan Xie, Xian-Hua Zhang, Rong-Bin Huang, Lan-Sun Zheng [1]

State Key Laboratory for Physical Chemistry of Solid Surfaces, Department of Chemistry, Xiamen University, Xiamen 361005, China

Abstract

By utilizing laser ablation, high purity trigonal selenium nanorods with different size have been synthesized from selenium powders. The high purity of the nanorods is attributed to freestanding growth process without catalyst or template. Its morphologies depend on both substrate temperature and reaction time. By controlling the experimental conditions, selenium nanorods with lateral dimensions in different range can be synthesized ranging from 20 nm to several hundred nanometers in width, and up to 10 μm in lengths.
© 2002 Elsevier Science B.V. All rights reserved.

Synthesis of nanoscale materials plays a critical role in understanding fundamental properties of small structures, creating nanostructured materials, and developing nanotechnologies [1–8]. One-dimensional or quasi-one-dimensional nanomaterials have received increasing attention due to their potential application in fabricating new types of nanoelectronic, optoelectronic, electrochemical, or electromechanical devices [9,10]. By utilizing of various synthetic technologies such as template [11,12], laser ablation [8,13,14], electrochemical fabrication [15,16], solution–liquid–solid growth [17], solution synthesis [18,19], solvothermal method [20] and other methods [21–23], efforts focusing on the bulk fabrication of nanowires or nanorods have achieved considerable advancements over the past several years. Among these methods, laser ablation is very attractive and efficient for the freestanding growth of nanowires in high yield under controllable experimental conditions. For example, the laser ablation method has been successfully applied in the synthesis of a broad range of multi-component semiconductor nanowires [8].

Due to its many useful properties, selenium has been of tremendous importance in a wide variety of applications [24–28]. As examples, trigonal selenium (t-Se) is known as a photoconductor with a spectral sensitivity covering almost the entire visible range [24], which makes selenium useful in the production of photocells and exposure meters for

---

* Corresponding author. Fax: +86-592-2183047.

E-mail addresses: zxxie@xmu.edu.cn (Z.-X. Xie), lszheng@ xmu.edu.cn (L.-S. Zheng).

[1] Also Corresponding author.

photographic application; selenium is also very important material in the Xerox machines and rectifiers [28]. It could be expected that the availability of selenium nanostructures should bring in new types of applications or enhance the performances of the currently existing devices as a result of quantum-sized effects [28]. However, only a few approaches have been reported to synthesis selenium nanowires, by using techniques of catalytic growth [26] and solution phase approach [27,28]. It is still a challenging research area to explore novel methods for the synthesis of one-dimensional selenium nanomaterials. Herein we report a laser ablation growth of high purity selenium nanorods with controlled size. This technique requires neither metal catalyst nor template, which is usually needed in many other methods, so as to simplify the purification process and to facilitate the subsequent application of the nanostructured products.

High-purity selenium (0.5 g) powders were added into the bottom of a quartz tube (35 cm length), which was vertically inserted into a tube furnace. Argon was introduced into the tube to keep off the O_2. Fundamental output of a Q-switched Nd:YAG laser (Quantary DCR 130), 1064 nm in wavelength and 7 ns in pulse width, was gently focused on the selenium by a long focal-length lens. A brick-red smoke immediately appeared in the tube and gradually deposited on the wall of the tube. During the growth of selenium on the tube wall, the tube was heated to a given temperature (background temperature) by the furnace, in which the value of the background temperature decreased gradually to the room temperature from the bottom to the open tip of the tube. After the laser ablation, the system was cooled down to the room temperature. The products were carefully collected according to the different colors, depending on their positions on the tube. The products were then washed with ethanol for further analysis.

On the wall of the quartz tube, four main color strips can be clearly distinguished. From the bottom to the open tip of the tube, with a decrease in temperature from ~300 °C to room temperature, the color changed from black gray to brown, dark red and brick red. Fig. 1 shows the transmission electron microscopy (TEM, JEM-100CXII) images of typical morphologies of the products collected according to the different colors of the deposits on the wall of the quartz tube. In the
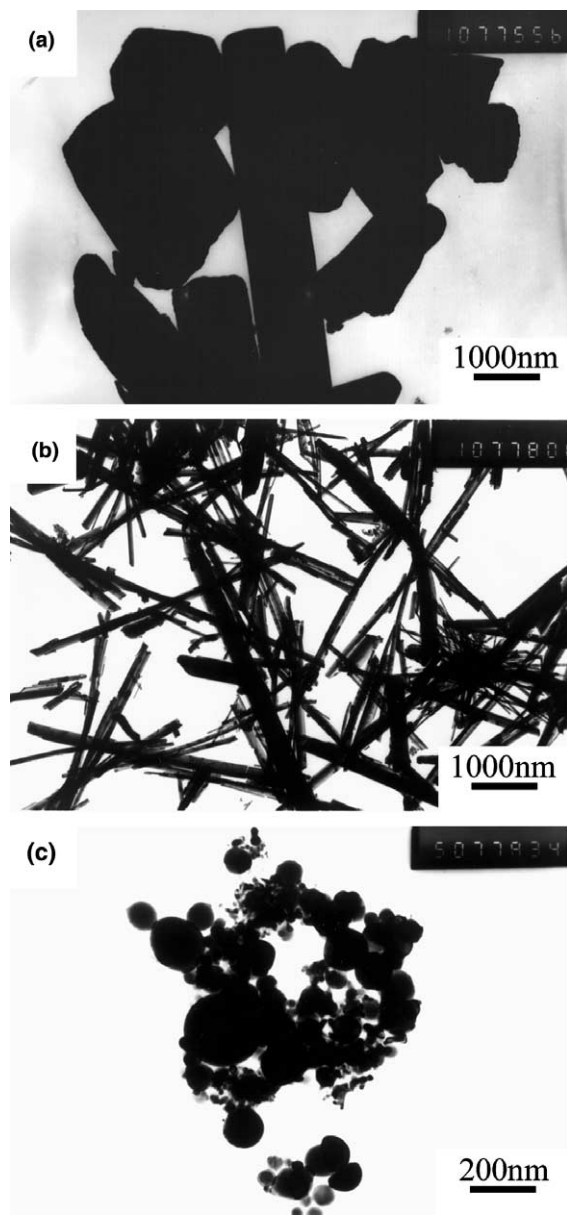

Fig. 1. Typical TEM images of the products collected in different colors zones, i.e., in different substrate temperature: (a) black gray zone (~300–220 °C), (b) brown to dark red zone (~220–110 °C), (c) brick red zone(less than 110 °C).

black gray zone (~300–220 °C), most of the deposits are particles and rods with different shape in micron-scale as shown in Fig. 1a. In the brown to dark red zone (~220–110 °C), all of the deposit are in rod-like shape as shown in Fig. 1b. The rods are about 20 to 300 nm in width and their lengths are up to tens micron. In Fig. 1c, the image of the products collected from the brick red zone is shown, indicating that most of the products are spherical particles with the diameter of tens nanometer, and there are also a few amorphous solids mixing with the spherical particles.

It can be seen from the Fig. 1 that the selenium grew into different shapes on the glass tube at different background temperatures. In order to get abundant uniform nanorods, the temperature of the glass tube was well controlled in the further experiment. Fig. 2a shows the TEM image of typical nanorods grown at the temperature of 170–120 °C. The abundant straight nanorods with the width of 30–80 nm and length up to 10 μm are clearly observed. Fig. 2b is a TEM image of one selenium nanorod of this product that has a length and width of ~3 μm and ~35 nm, respectively. The microdiffraction pattern inserted in the figure was recorded by directing the electron beam onto this particular nanorod, showing a single-crystalline diffraction pattern. The diffraction pattern remained essentially the same when the focused e-beam spot was scanned along the nanorod. It could be deduced that the selenium nanorods synthesized using the present approach were single-crystalline. By TEM observation, the synthesized selenium nanorods were found structurally stable in air over periods of several months. The X-ray diffraction pattern (XRD, Cu K_α radiation) of these products is shown in Fig. 3a. All of the peaks could be indexed as the trigonal phase of selenium (JCPDS CARDS No. 06-0362). The peaks are obviously broadened, due to the small dimensions of these nanorods. The purity of as-synthesized selenium nanorods was also confirmed by the XPS characterization (Fig. 3b). The strong peak at 55.2 eV corresponds to selenium $3d_{5/2}$ binding energy for Se^0. The Raman scattering spectrum (Fig. 3c) shows a strong peak at ~234 cm^{-1}, which corresponds to the characteristic stretching mode of a

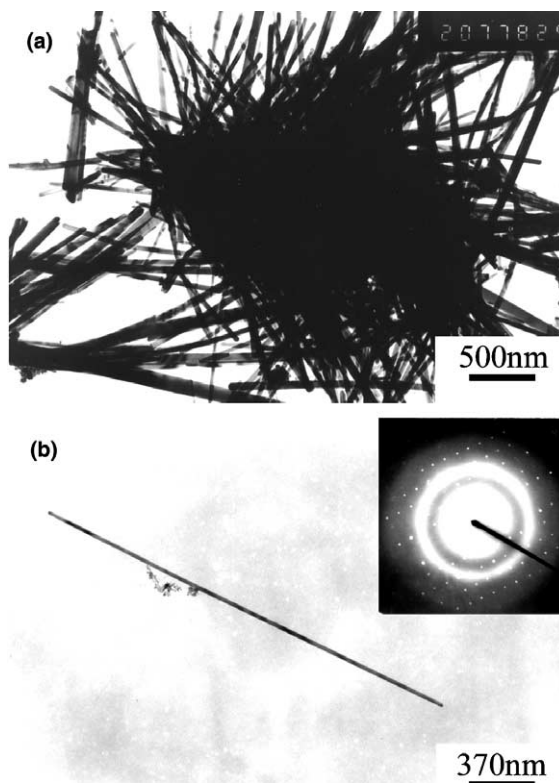Fig. 2. (a) TEM image of selenium nanorods grown at the temperature of 170–120 °C. (b) TEM image of one as-prepared selenium nanorod and its electron diffraction pattern (inserted in the corner of the figure).

chain-like structure that only exists in the trigonal phase [29].

It should also be pointed out that without the assisting of laser, no nanorods are observed in our experiments, and the time of the laser ablation is an important factor for the growth of the selenium rods. A typical ablation time is 10–20 min. A shorter ablation time results in the products with a smaller lateral dimension and a less yield. On the other hand, overlong reaction time makes the selenium nanorods aggregate.

From the TEM results as shown in Fig. 1, it can be deduced that the morphology of the selenium grown on the tube wall depends on the temperature of the substrate. While the selenium sample was ablated by the laser beam, selenium was evaporated from the bottom of the tube and its vapor
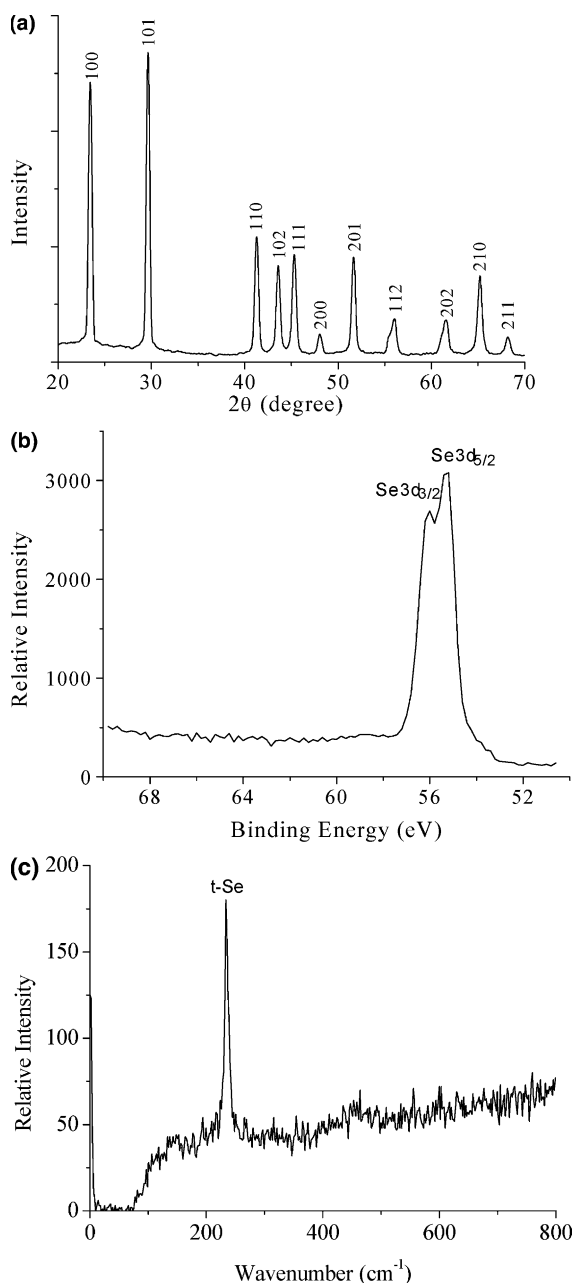
(a)

(b)

(c)

Fig. 3. (a) XRD pattern, (b) XPS pattern and (c) Raman scattering spectrum of the as-prepared selenium nanorods with diameter of ∼30–80 nm.

filled in the quartz tube. Understandably, selenium gas would segregate into different types at the different parts of the tube, where the temperatures are different. The melting point of selenium is 217 °C. At the bottom part of the tube, the temperature is over 220 °C, which is higher than the melting point of selenium. The selenium gas will segregate into selenium liquid droplet. The liquid droplets deposit on tube wall and grow larger and larger. As the tube was cooled down to the room temperature after laser ablation, the selenium liquid droplet on the tube wall solidified and crystallized into different shapes (see Fig. 1a). At the place where the temperature is about the melting point or a little bit lower than the melting point, the selenium vapor will segregate and solidified on the tube wall. Since the melting point of nanoparticles decreases with the decreasing size in the range of nanometer, selenium vapor might underwent the formation of nano-droplets and then solidified to nano-crystals on the tube wall, although the background temperature was lower than the melting point of selenium. In this process, the background temperature affected the size of selenium nano-droplets and defined the size of the selenium nano-crystals. Further selenium vapor continued to adsorb on the selenium nano-crystals and crystallized, resulting in the one-dimensional growth of crystalline selenium nanorods. As a result, higher background temperature produced larger selenium nanorods, since larger selenium nano-droplets could only exist at higher temperature. Therefore, relatively small and uniform selenium nanorods were obtained at the background temperature range of 120–170 °C as shown in Fig. 2. From the micro-diffraction of selenium nanorod (Fig. 2b), it could be found that the two-fold rotational symmetry existed in this pattern, suggesting that the *c*-axis is along the rod. The nanorods grew along the helical chains and the *c*-axis characterizes selenium crystals. When the background temperature is too low, however, the selenium vapor will segregate and form nanoparticles, which then directly deposit on the tube wall. Therefore, at the top of the tube where was at room temperature, spheric nanoparticles and amorphous solids were formed and observed (see Fig. 1c).

Selenium nanorods have been successfully synthesized by several groups. By using silver colloids as seeds, selenium rods in the size of micrometer can be grown from an aqueous dispersion of α-Se

colloids [26]. However, to remove the silver catalysts could be a problem. By one-dimensional assemblage, A. Abdelouas et al. [27] have fabricated selenium nanowires through reducing SeO_4^{2-} in the solution, but most of the products were in fact chainlike aggregates of nanoparticles of monoclinic selenium. Another successful way to synthesize the selenium nanowires was by a solution phase approach [28], in which colloidal particles of amorphous (α-)Se were converted into wires with diameters of 10–30 nm and lengths up to hundreds of microns. However, a relatively long aged time (10 days) was required. By the laser ablation as described in this paper, the synthesis of selenium nanorods required no catalyst or template. Furthermore, the morphology and the dimension of the products can be controlled.

In summary, nano-structured selenium products with different shapes have been synthesized from selenium powders by laser ablation. By controlling the temperature in the reactor, selenium nanorods with lateral dimensions in different range can be selectively and abundantly produced ranging from 20 nm to several hundred nanometers, and the length of selenium nanorods can be up to tens of micron. The selenium nanorods synthesized by the proposed method are free from any catalyst or template, which is benefit to the further use.

Acknowledgements

References

[1] C.B. Murray, C.R. Kagan, M.G. Bawendi, Science 270 (1995) 1335.

[2] A.P. Alivisatos, Science 271 (1996) 933.

[3] C.P. Collier, T. Vossmeyer, J.R. Heath, Annu. Rev. Phys. Chem. 49 (1998) 371.

[4] C.M. Lieber, Solid State Commun. 107 (1998) 106.

[5] B.I. Yacobson, R.E. Smalley, Am. Sci. 85 (1997) 324.

[6] J. Hu, T.W. Odom, C.M. Lieber, Acc. Chem. Res. 32 (1999) 435.

[7] D. Snoke, Science 273 (1996) 1351.

[8] X.F. Duan, C.M. Lieber, Adv. Mater. 12 (2000) 298.

[9] S.M. Prokes, K.L. Wang, MRS Bull. 24 (1999) 13.

[10] B. Mayers, B. Gates, Y.D. Yin, Y.N. Xia, Adv. Mater. 13 (2001) 1380.

[11] E. Braun, Y. Eichen, U. Sivan, G. Ben-Yoseph, Nature 391 (1998) 775.

[12] J. Sloan, D.M. Wright, H.G. Woo, S. Bailey, G. Brown, A.P.E. York, K.S. Coleman, J.L. Hutchison, M.L.H. Green, Chem. Commun. (1999) 699.

[13] A.M. Morales, C.M. Lieber, Science 279 (1998) 208.

[14] W.S. Shi, Y.F. Zheng, N. Wang, C.S. Lee, S.T. Lee, Adv. Mater. 13 (2001) 591.

[15] M.P. Zach, K.H. Ng, R.M. Penner, Science 290 (2000) 2120.

[16] X.Y. Zhang, L.D. Zhang, W. Chen, G.W. Meng, M.J. Zheng, L.X. Zhao, Chem. Mater. 13 (2001) 2511.

[17] H.F. Yan, Y.J. Xing, Q.L. Hang, D.P. Yu, Y.P. Wang, J. Xu, Z.H. Xi, S.Q. Feng, Chem. Phys. Lett. 323 (2000) 224.

[18] C.C. Chen, C.Y. Chao, Z.H. Lang, Chem. Mater. 12 (2000) 1516.

[19] J.D. Holmes, K.P. Johnston, R.C. Doty, B.A. Korgel, Science 287 (2000) 1471.

[20] J. Yang, J.H. Zeng, S.H. Yu, L. Yang, G.E. Zhou, Y.T. Qian, Chem. Mater. 12 (2000) 3259.

[21] Y.Y. Wu, P.D. Yang, Chem. Mater. 12 (2000) 605.

[22] M. He, I. Minus, P.Z. Zhou, S.N. Mohammed, J.B. Halpern, R. Jacobs, W.L. Sarney, L. Salamanca-Riba, R.D. Vispute, Appl. Phys. Lett. 77 (2000) 3731.

[23] S.W. Liu, J. Yue, A. Gadanken, Adv. Mater. 13 (2001) 656.

[24] N.I. Ibragimov, Z.M. Abutalibova, V.G. Agaev, Thin Solid Films 359 (2000) 125.

[25] B. Pejova, I. Grozdanov, Appl. Surf. Sci. 177 (2001) 152.

[26] J.-P. Lickes, F. Dumont, C. Buess-Herman, Colloids Surf. A 118 (1996) 167.

[27] A. Abdelouas, W.L. Gong, W. Lutze, J.A. Shelnutt, R. Franco, I. Moura, Chem. Mater. 12 (2000) 1510.

[28] B. Gates, Y.D. Yin, Y.N. Xia, J. Am. Chem. Soc. 122 (2000) 12582.

[29] V.V. Poborchii, A.V. Kolobov, J. Caro, V.V. Zhuravlev, K. Tanaka, Chem. Phys. Lett. 280 (1997) 17.